J Mater Sci (2017) 52:10387–10392

Energy materials

Quantification of germanium-induced suppression of interstitial injection during oxidation of silicon

Thomas P. Martin[1,*], K. S. Jones[1], Renata A. Camillo-Castillo[2,6], Christopher Hatem[3], Yan Xin[4], and Robert G. Elliman[5]

[1] Department of Materials Science and Engineering, University of Florida, Gainesville, FL 32611, USA
[2] RF Technology Development, GlobalFoundries 1000 River Road, Essex Junction, VT 05452, USA
[3] Applied Materials Varian Semiconductors, Gloucester, MA 01930, USA
[4] National High Magnetic Field Laboratory, Florida State University, Tallahassee, FL 32310, USA
[5] Department of Electronic Materials Engineering, Research School of Physics and Engineering, The Australian National University, Canberra, ACT 2601, Australia
[6] Present address: Intel Corporation, Hillsboro, OR, USA

Received: 30 January 2017
Accepted: 10 May 2017
Published online: 22 May 2017

© Springer Science+Business Media New York 2017

ABSTRACT

The oxidation of silicon is known to inject interstitials, and the presence of silicon–germanium (SiGe) alloys at the Si/SiO_2 interface during oxidation is known to suppress the injection of silicon self-interstitials. This study uses a layer of implantation-induced dislocation loops to measure interstitial injection as a function of SiGe layer thickness. The loops were introduced by a 50 keV 2×10^{14} cm^{-2} P^+ room-temperature implantation and thermal annealing. Germanium was subsequently introduced via a second implant at 3 keV Ge^+ over a range of doses between 1.7×10^{14} cm^{-2} and 1.4×10^{15} cm^{-2}. Results show that upon oxidizing at 850 °C for 3 h or 900 °C for 70 min to condense the germanium at the Si/SiO_2 interface, where if forms a $Si_{0.5}Ge_{0.5}$ alloy. Upon subsequent oxidations of 850 °C for 6 h or 900 °C for 2 h, partial suppression of interstitial injection can be observed for sub-monolayer doses of germanium, and more than three monolayers of $Si_{0.5}Ge_{0.5}$ (1.4×10^{15} cm^{-2}) are necessary to suppress interstitial injection below the detection limit during oxidation. These results show that low-energy implantation of germanium can be used to eliminate or modulate injection of oxidation-induced interstitials.

Introduction

Silicon–germanium (SiGe) is known to suppress the injection of silicon self-interstitials into the substrate during the oxidation of silicon [1, 2]. These interstitials are believed to arise from the volume mismatch between silicon and the oxide, wherein one unit volume of silicon produces 2.25 unit volumes of oxide [3]. The mechanism by which germanium suppresses this phenomenon is still open to debate

Address correspondence to E-mail: tmartin512@ufl.edu

DOI 10.1007/s10853-017-1196-1

with the three competing theories being that: the germanium reduces interstitial formation by being more closely lattice matched with the oxide (thus reducing interstitial generation) [4], that the formation energy of creating an interstitial in the SiGe lattice is higher than in pure Si [5], thus driving all the excess interstitials into the oxide rather than the substrate, or that the presence of Ge at the interface alters the stepwise mechanism of the oxidation reaction in some way [6]. Despite uncertainty about the mechanism, it is widely believed that only the first monolayer at the oxidizing interface is sufficient to account for the germanium effects on oxidation [7–9]. Experimentally, $Si_{0.5}Ge_{0.5}$ layers as thin as 50 Å have been shown to totally suppress interstitial injection during an oxidation, but nothing is known about thinner layers, although it has been suggested that a brief initial transient pileup stage may be required to achieve interstitial suppression [9, 10]. Most previous studies have reported total suppression when germanium is present at the Si/SiO_2 interface, making it difficult to study. The goal of this work is to study how controlling the dose of Ge at the surface in the sub-monolayer to several monolayers regime affects the injection of interstitials during the oxidation of silicon.

Materials and methods

Silicon wafers were implanted at room temperature with 50 keV phosphorus ions to a dose of 2×10^{14} cm^{-2} then subjected to a 750 °C furnace anneal for 30 min under argon ambient to nucleate sub-threshold dislocation loops. Subsequently, 30 nm of silicon was epitaxially grown at ~600 °C by MOCVD [11, 12], increasing the depth of the loop layer to 100 nm. Next the Ge samples were implanted at room temperature with 3 keV germanium ions to various doses. The doses used were designed to correspond to fractions of the areal atomic density of the silicon (100) surface and were 1.7×10^{14} cm^{-2}, 3.4×10^{14} cm^{-2}, 5.1×10^{14} cm^{-2}, 6.8×10^{14} cm^{-2}, and 1.4×10^{15} cm^{-2}, corresponding to 0.25, 0.5, 0.75, 1, and 2 monolayers of pure Ge, respectively. These implants produced a thin amorphous layer, but no extended defects are formed for implants at this energy [13]. In order to pile up the implanted germanium at the active interface and probe its effect, a condensation step first had to be performed by oxidizing through the implant range of the Ge^+ implant as shown in Fig. 1a and b. A germanium layer away from the oxidizing interface presents no barrier to interstitial movement, so it was essential that all implanted Ge be at the active interface [14].

Two different temperatures, 850 °C and 900 °C, were studied. For the 850 °C samples, condensation anneals were performed for 3 h followed by 6 h anneals at 850 °C. For the 900 °C samples the condensation step was 70 min followed by 2 h further oxidation. These anneals were performed in a tube furnace operating under a pure O_2 ambient. Following the condensation annealing, the effect of subsequent oxidation on Ge accumulation and interstitial injection was studied.

Results and discussion

It is well known that implanted germanium can be segregated at an oxidizing Si interface to form a pseudomorphic Ge-rich SiGe layer at the interface [7]; however, its effects on interstitial injection have never been studied for such small Ge concentrations. In addition, these earlier studies [7, 8] used higher Ge doses and energies and did not attempt to quantify segregation at the sub-monolayer level. Therefore, it was important to verify that the entire implant dose was segregated to the SiO_2/Si interface in the present case. For this, high-angle annular dark field scanning transmission electron microscopy (HAADF-STEM) imaging technique was used to image both oxidized samples HAADF-STEM images were acquired on a JEM-ARM200cF at 200 kV with a 0.078 nm resolution, a beam semi-convergence angle of 22 mrad, and a 78 mrad collection angle. The results are shown in Fig. 2.

Since Ge has a higher atomic number than Si, the dumbbells of $Si_{1-x}Ge_x$ alloy should exhibit brighter contrast in the HAADF_STEM images. Both images of the two samples with different annealing time (Fig. 2a, b) show two bright dumbbell layers at the surface, corresponding to roughly four monolayers on a Si {100} surface. According to theory [15], the germanium should condense to an equilibrium value of $Si_{0.5}Ge_{0.5}$ at 850 °C, which would correspond to four layers of Ge-enriched material if the entire dose is present. This is exactly what is observed in Fig. 2, suggesting that none of the Ge is lost to mixed oxide formation early in the oxidation process [16].

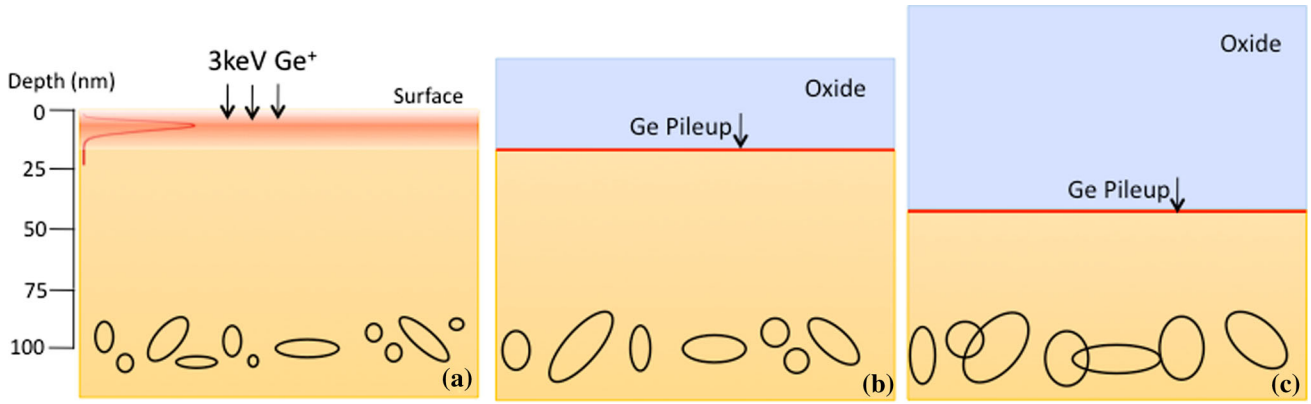

Figure 1 Schematic diagram of the experimental setup showing **a** the samples post-implant, **b** the samples following the condensation anneal, and **c** the samples following subsequent oxide growth. The *black* circles at 100 nm representing loops can be seen to both coarsen and grow in response to these anneals.

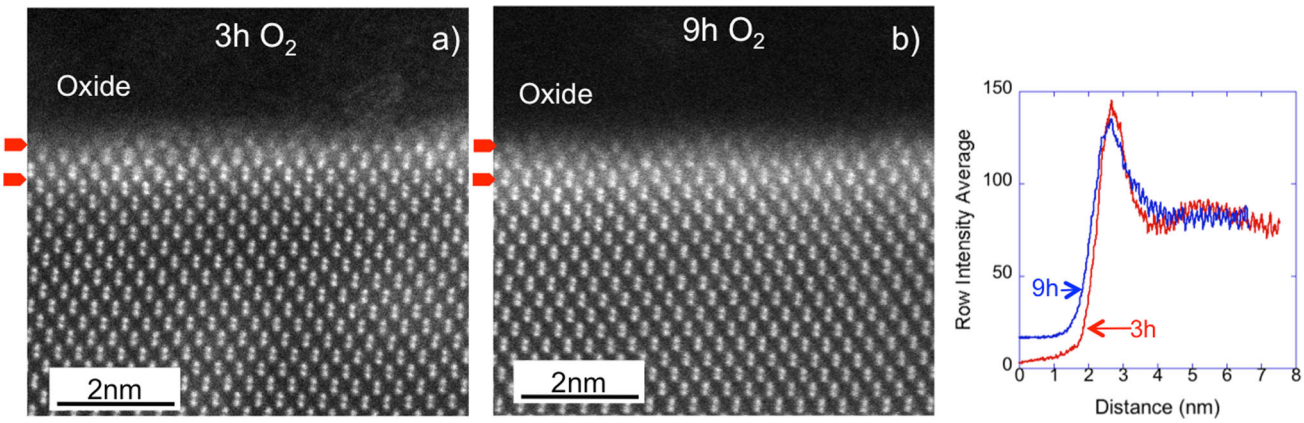

Figure 2 **a** HAADF-STEM image of a sample with 3 keV, 1.4×10^{15} cm^{-2} Ge^+ implant followed by a 3 h 850 °C furnace annealing under dry O_2. **b** HAADF-STEM image of the same sample followed by a 9 h annealing under the same conditions. **c** Comparison of image intensity when normalized for background and intensity onset. This shows little to no peak broadening.

In order to quantify the degree of interstitial suppression caused by the Ge, the buried dislocation loops from the previous phosphorus implant and anneal were used as detectors. It is well known that a layer of such loops can be used to trap a flux of interstitials provided that their planar density is $>1 \times 10^{10}$ cm^{-2}, while our density was a minimum of 2×10^{10} cm^{-2} even after thermal coarsening [17]. The subsequent growth of the loops can then be used to quantify the number of interstitials injected [17, 18]. PTEM samples were made using a polish and etch process and imaged in weak-beam dark-field (WBDF) conditions. The loop density and total number of bound interstitials were then quantified [19, 20].

Figure 3 shows the number of trapped interstitials in the loops after annealing in inert and oxidizing ambients as a function of Ge dose. By subtracting the inert value from the oxidized value, one can determine the net interstitial injection due to oxidation. As the Ge dose increases, the number of injected interstitials also decreases. By fitting an exponential to our data as in Fig. 4, we can extrapolate that the injection would likely drop below our detection limit for Ge doses above or around 3×10^{15} cm^{-2}. This corresponds to around 8.8 layers of $Si_{0.5}Ge_{0.5}$ at the interface. The data also show that even a very small amount of germanium present at the active interface is sufficient to induce a measurable and significant drop in interstitial injection.

Figure 4 shows that germanium is more effective at suppressing interstitial injection at lower temperatures, but that the suppression behavior follows a similar exponential decrease with increasing Ge concentration for both temperatures. Contrary to previous assumptions that only one monolayer was

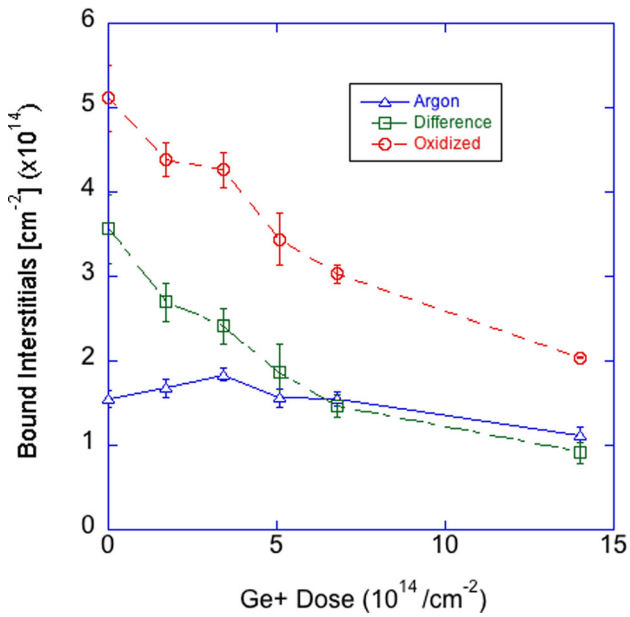

Figure 3 Bound interstitial areal density as a function of Ge dose for the annealing performed at 850 °C. The *lower* line (*triangular markers*) represents control samples annealed in an inert (argon) ambient, the *upper* line (*circular markers*) represents the data for oxidized samples, and the line in the *middle* (*square markers*) is the net injection during the post-condensation anneal.

necessary, this work shows that a single surface layer is insufficient, and our extrapolated data predict that around 3 monolayers of pure Ge, forming 6 monolayers $Si_{0.5}Ge_{0.5}$, would be needed at 850 °C and that nearly 5 monolayers of pure Ge forming almost 9 monolayers of $Si_{0.5}Ge_{0.5}$ would be needed at 900 °C to suppress interstitial injection to below our detection limit. Since in practice the germanium is piling up to only around 50%, this leads to thickness dependence [15]. Computational studies have shown that it is far less favorable to form silicon interstitial in $Si_{0.5}Ge_{0.5}$ but that does not explain the thickness dependence observed here as only the top layer should participate in the initial oxidation reaction and subsequent formation [10]. Microscopic segregation at the surface is a potential source of Si interstitials, but was not observed [4, 21, 22]. Nucleation events involving multiple layers are possible sources of thickness dependence, but were not observed [21–23]. However, it is important to note that if nanoscale segregation were taking place, the techniques used here would not have detected it. It is also possible that SiO_2 itself is able to penetrate a short distance into the substrate and participate in redox reactions with the

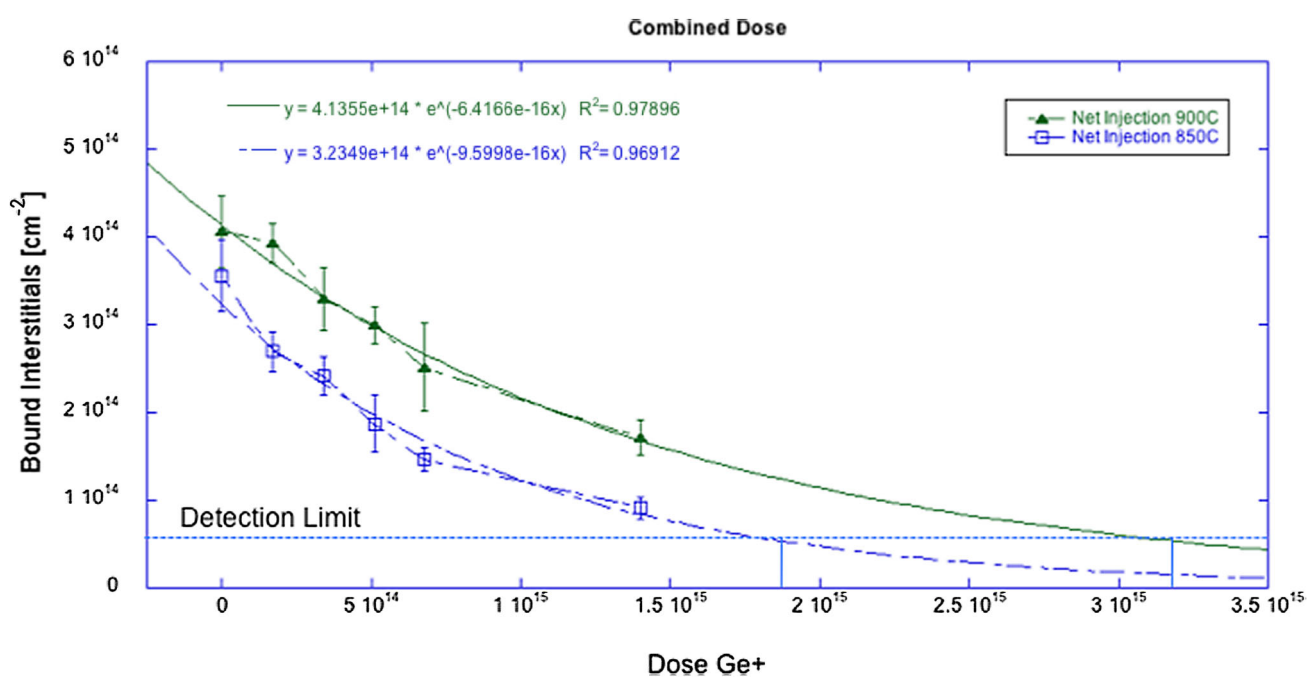

Figure 4 Combined net interstitial injection for 850 and 900 °C anneals. Interstitial injection clearly decreases exponentially with increasing Ge dose in both cases. Curve fitting gives R^2 values of 0.98 and 0.97 for the 900 and 850 °C anneals, respectively. Extrapolated detection limit for both curves is also shown.

silicon and germanium as GeO and SiO are both volatile species [24, 25]. This would be consistent with a reaction zone where SiGe must be fully present to have the shutoff effect [26, 27]. It is also speculated that the SiGe layer could act as a reservoir for Si interstitials, due to their slow passage through the layer. That is, the Si interstitials may simply never catch up with the advancing SiGe/Si interface and thus become incorporated into the SiGe layer instead. If this were the case, the effect would be more dramatic with increasing SiGe thickness and lower temperature, which is exactly what is observed. This could be tested by performing an inert annealing following an oxidizing annealing to see whether interstitial injection continues. Unfortunately, such a study would likely fall below the detection limit ($1 \times 10^{13}\text{cm}^{-2}$) of our loop detector technique. Further studies including DFT calculations are in progress to ascertain the mechanism, as structural changes upon addition of a phase can play an important role in observed effects [28]. Regardless of the exact mechanism, the ability to tailor interstitial injection during an oxidation using standard implant technology opens up new and unique processing windows.

Conclusion

Germanium remains active at an oxidizing interface well below the first layer, contrary to what was previously thought, that only the first layer of SiGe participated in oxidation reactions. This work has shown that far more than the surface layer participates in the interstitial suppression effects and that even very low concentration doping at the interface can have a dramatic and tunable affect on interstitial injection [7–9]. While the exact mechanism for this remains a subject of ongoing research, it should be possible to use this technique for such things as to tailor junction depths in deep devices provided the exponential functions extracted from our data can be extrapolated to tailor injection behavior in other dose and energy conditions not yet studied.

Acknowledgements

TEM work was performed at the National High Magnetic Field Laboratory, which is supported by NSF DMR-1157490 and the State of Florida. As well as the University of Florida Research Services Center.

Compliance with ethical standards

Conflict of interest The authors of this work declare they have no conflict of interest.

References

[1] LeGoues FK, Rosenberg R, Meyerson BS (1989) Kinetics and mechanism of oxidation of SiGe: dry versus wet oxidation. Appl Phys Lett 54:644–654. doi:10.1063/1.100905

[2] Jain SC, Balk P (1993) Preparation and properties of the GeSi-oxide system. Thin Solid Films 223:348–357. doi:10.1016/0040-6090(93)90543-x

[3] Hu S (1994) Nonequilibrium point defects and diffusion in silicon. Mater Sci Eng R Rep 13:105–192. doi:10.1016/0927-796X(94)90009-4

[4] Hu SM (1974) Formation of stacking faults and enhanced diffusion in the oxidation of silicon. J Appl Phys 45:1567–1568. doi:10.1063/1.1663459

[5] Delugas P, Fiorentini V (2004) Energetics of transient enhanced diffusion of boron in Ge and SiGe. Phys Rev B 69:085203–085205. doi:10.1103/PhysRevB.69.085203

[6] Tiller WA (1981) On the kinetics of the thermal oxidation of silicon III. Coupling with other key phenomena. J Electrochem Soc 128:689–697. doi:10.1149/1.2127482

[7] Fathy D, Holland OW, White CW (1987) Formation of epitaxial layers of Ge on Si substrates by Ge implantation and oxidation. Appl Phys Lett 51:1337–1344. doi:10.1063/1.98671

[8] Holland OW, White CW, Fathy D (1987) Novel oxidation process in Ge + -implanted Si and its effect on oxidation kinetics. Appl Phys Lett 51:520–524. doi:10.1063/1.98385

[9] LeGoues FK, Rosenberg R, Meyerson BS (1989) Dopant redistribution during oxidation of SiGe. Appl Phys Lett 54:751–754. doi:10.1063/1.100882

[10] Napolitani E, Di Marino M, De Salvador D et al (2005) Silicon interstitial injection during dry oxidation of SiGe/Si layers. J Appl Phys 97:036106–036113. doi:10.1063/1.1844606

[11] Meyerson BS (1986) Low-temperature silicon epitaxy by ultrahigh vacuum/chemical vapor deposition. Appl Phys Lett 48:797. doi:10.1063/1.96673

[12] Harame DL, Meyerson BS (2001) The early history of IBM's SiGe mixed signal technology. IEEE Trans Electron Devices 48:2555–2567. doi:10.1109/16.960383

[13] Claverie A, Colombeau B, de Mauduit B et al (2003) Extended defects in shallow implants. Appl Phys A 76:1025–1033. doi:10.1007/s00339-002-1944-0

[14] Martin TP, Aldridge HL Jr, Jones KS, Camillo-Castillo RA (2017) Use of a buried loop layer as a detector of interstitial flux during oxidation of SiGe heterostructures. J Vac Sci Technol, A 35:021101–021105. doi:10.1116/1.4972516

[15] Long E, Azarov A, Kløw F et al (2012) Ge redistribution in SiO2/SiGe structures under thermal oxidation: dynamics and predictions. J Appl Phys 111:024308–024310. doi:10.1063/1.3677987

[16] Hellberg PE, Zhang SL, d'Heurle FM, Petersson CS (1997) Oxidation of silicon–germanium alloys. I. An experimental study. J Appl Phys 82:5773–5777. doi:10.1063/1.366443

[17] Listebarger JK, Jones KS, Slinkman JA (1993) Use of type II (end of range) damage as "'detectors'" for quantifying interstitial fluxes in ion-implanted silicon. J Appl Phys 73:4815–4816. doi:10.1063/1.353847

[18] Jones KS, Robinson HG, Listebarger J et al (1995) Studies of point defect/dislocation loop interaction processes in silicon. Nucl Instrum Methods Phys Res Sect B Beam Interact Mater At 96:196–201. doi:10.1016/0168-583x(94)00482-x

[19] Ratib O, Rosset A (2006) Open-source software in medical imaging: development of OsiriX. Int J CARS 1:187–196. doi:10.1007/s11548-006-0056-2

[20] Rosset A, Spadola L, Ratib O (2004) OsiriX: an open-source software for navigating in multidimensional DICOM images. J Digit Imaging 17:205–216. doi:10.1007/s10278-004-1014-6

[21] Aqua JN, Berbezier I, Favre L et al (2013) Growth and self-organization of SiGe nanostructures. Phys Rep 522:59–189. doi:10.1016/j.physrep.2012.09.006

[22] Kaplan WD, Chatain D, Wynblatt P, Carter WC (2013) A review of wetting versus adsorption, complexions, and related phenomena: the rosetta stone of wetting. J Mater Sci 48:5681–5717. doi:10.1007/s10853-013-7462-y

[23] Watanabe H, Baba T, Ichikawa M (2000) Mechanism of layer-by-layer oxidation of Si(001) surfaces by two-dimensional oxide-island nucleation at SiO 2/Si interfaces. Jpn J Appl Phys 39:2015–2020. doi:10.1143/jjap.39.2015

[24] Elliman RG, Kim TH, Shalav A, Fletcher NH (2012) Controlled lateral growth of silica nanowires and coaxial nanowire heterostructures. J Phys Chem C 116:3329–3333. doi:10.1021/jp208484y

[25] Uematsu M, Gunji M, Tsuchiya M, Itoh KM (2007) Enhanced oxygen exchange near the oxide/silicon interface during silicon thermal oxidation. Thin Solid Films 515:6596–6600. doi:10.1016/j.tsf.2006.11.052

[26] Kageshima H, Uematsu M, Shiraishi K (2001) Theory of thermal Si oxide growth rate taking into account interfacial Si emission effects. Microelectron Eng 59:301–309. doi:10.1016/S0167-9317(01)00614-1

[27] Estève A, Rouhani MD, Faurous P, Esteve D (2000) Modeling of the silicon (100) thermal oxidation: from quantum to macroscopic formulation. Mater Sci Semicond Process 3:47–57. doi:10.1016/s1369-8001(00)00009-3

[28] Reifsnider K, Rabbi F, Vadlamudi V et al (2017) Critical path-driven property and performance transitions in heterogeneous microstructures. J Mater Sci 52:4796–4809. doi:10.1007/s10853-017-0791-5